Available online at www.sciencedirect.com

SCIENCE DIRECT®

Journal of Molecular Catalysis A: Chemical 202 (2003) 239–246

JOURNAL OF MOLECULAR CATALYSIS A: CHEMICAL

www.elsevier.com/locate/molcata

W/HZSM-5 catalyst for methane dehydroaromatization: a multinuclear MAS NMR study

Jun Yang, Feng Deng*, Mingjin Zhang, Qing Luo, Chaohui Ye

[a] *State Key Laboratory of Magnetic Resonance and Atomic and Molecular Physics, Wuhan Institute of Physics and Mathematics, The Chinese Academy of Sciences, Wuhan 430071, PR China*

Received 18 September 2002; received in revised form 28 February 2003; accepted 10 March 2003

Abstract

Multinuclear solid-state NMR techniques were employed to investigate the interaction between tungsten species and zeolite in W/HZSM-5 catalysts prepared by controlled impregnation. ^{27}Al, ^{29}Si NMR experiments suggest that introduction of W species leads to the formation of distorted four-coordinate framework and six-coordinate extra-framework aluminum species due to the interaction of the W species and framework aluminum, and the former can be further transformed into the latter, especially at high W loadings. ^{1}H MAS NMR indicates that some of the W species disperse on the external surface and some of them diffuse into the internal channels of the zeolite, which causes a decrease of the Brönsted acid sites and silanols as well as an increase of the extra-framework Al–OH species in the W/HZSM-5 catalysts. Cooperation of the W species and the remaining Brönsted acid sites is responsible for the activity of the W/HZAM-5 catalysts for methane dehydroaromatization. As revealed by ^{13}C NMR experiments, an induction period exists for methane dehydroaromatization reaction and W^{6+} oxide on/in the zeolite is likely to be converted into W^{4+} oxide during the reaction. It is W^{4+} oxide rather than carbide tungsten that acts as active metal sites for initial activation of methane on the W/HZSM-5 catalysts.
© 2003 Elsevier Science B.V. All rights reserved.

Keywords: Methane activation; Solid-state NMR; W/HZSM-5; Active metal phase; Bifunctional catalyst

1. Introduction

Methane, as a principal component of natural gas, is considered as a potential resource for energy and chemical production in this century [1]. Ever since the last century, great efforts have been made in effective utilization of methane, from practical and theoretical points of views. In 1993, Xu and co-workers [2] first reported that methane could be transformed into aromatics under non-oxidative condition at 973 K and atmospheric pressure with approximately 10% methane conversion and high aromatics selectivity by using molybdenum modified HZSM-5 catalyst. Since then, this catalyst/reaction has been investigated from various aspects [3–11]. FT-IR [4,5], XPS [3], EPR [8], ISS [3], MAS NMR [9,10] and other techniques [11] have been used to characterize the interaction between Mo and zeolite HZSM-5, to elucidate the nature of Mo species, which relates to the formation of active metal phase, and to explore the mechanism of reaction. At present, it is generally accepted that Brönsted acid sites and channels of zeolite as well as carbide molybdenum are crucial factors for the catalytic performance of the catalyst.

However, Mo/HZSM-5 based catalysts, operating at about 973 K, give a low methane conversion (ca.

* Corresponding author. Tel.: +86-27-8719-8820; fax: +86-27-9819-9291.
E-mail address: dengf@wipm.ac.cn (F. Deng).

1381-1169/03/$ – see front matter © 2003 Elsevier Science B.V. All rights reserved.
doi:10.1016/S1381-1169(03)00187-0

10%) because of the thermodynamic limit. It is predicted that an operation temperature as high as 1073 K is required for about 20% methane conversion. However, at such high temperature, Mo-based catalysts suffer from serious loss of Mo component due to the sublimation. Recently, Zhang and co-workers [12] reported highly active and heat-resisted W/HZSM-5 based catalysts for methane dehydroaromatization. Operating at 1073 K and under atmospheric pressure, it gains a methane conversion about 20% with high benzene selectivity and without the loss of W species. The methane conversion is approaching the level that might be commercially attractive for the production of aromatics from methane. As a bifunctional catalyst, Brönsted acid sites and W species are crucial to catalytic performance, but some important aspects of the catalyst/reaction are not investigated, such as the distribution of the W species in/on zeolite, the variation of acidity and structure of zeolite due to the interaction between W species and HZSM-5, and the active metal phase for initial activation of methane. Solid-state NMR has proved to be a powerful technique for investigating the structure of various solid catalysts [13,14] and the reaction mechanism [15,16]. In the present work, we used multinuclear MAS NMR techniques such as ^{27}Al, ^{29}Si, ^{1}H MAS and ^{1}H → ^{27}Al, ^{1}H → ^{29}Si CP/MAS NMR, to characterize the W/HZSM-5 catalyst so as to reveal the interaction between W species and HZSM-5 zeolite support. In addition, we also studied the methane dehydroaromatization reaction on the catalyst by ^{13}C MAS NMR spectroscopy.

2. Experimental

2.1. Samples preparation

A series of W/HZSM-5 catalysts were prepared according to the procedure described in the literature [12]: HZSM-5 powder was impregnated with an aqueous solution containing a given amount of ammonium tungstate ($(NH_4)_5H_5[H_2(WO_4)_6]\cdot H_2O$) and the pH value of the solution was regulated to 2–3 by H_2SO_4. The mixture was dried at room temperature for 12 h, at 373 K for 8 h and then calcined at 773 K for 5 h. W/HZSM-5 with different W loadings were denoted as *x*W/HZSM-5, where *x* is the weight percentage of the W content in the sample.

Prior to ^{27}Al MAS and ^{1}H → ^{27}Al CP/MAS NMR measurements, the samples were rehydrated completely in a desiccator containing saturated NH_4NO_3 solution. Prior to ^{1}H MAS and ^{1}H{^{27}Al} TRAPDOR NMR experiments, the samples were dehydrated at 673 K under pressure below 10^{-3} Pa for 5 h on a vacuum line and finally sealed in glass tubes.

About 0.5 g 4W/HZSM-5 power was placed into a quartz tube, and activated in vacuum (10^{-3} Pa) at 673 K for 5 h. Methane (^{13}C, 99%, Cambridge Isotope Inc.) was introduced and frozen on the catalyst under vacuum with liquid N_2 and then the quartz tube was sealed. The pressure in quartz tube was about 1 atm. The sealed ampule was heated at different temperatures for a specific period and then the reaction was quenched by liquid N_2. Prior to ^{13}C NMR measurement, all sealed ampules were opened and the samples were transferred into a ZrO_2 rotor (tightly sealed by a Kel-F cap) under a dry nitrogen atmosphere in a glove box.

2.2. NMR experiments

All the NMR experiments were carried out at 9.4 T on a Varian Infinityplus-400 spectrometer. ^{27}Al MAS NMR spectra were recorded with a 4 mm probe at 105.4 MHz using a 0.7 μs ($<\pi/12$) pulse, a 0.5 s recycle delay, and a 10 kHz spinning rate. ^{1}H → ^{27}Al CP/MAS NMR experiments were measured with a single contact time of 1 ms, a 2 s recycle delay and a 5 kHz spinning rate. The Hartmann–Hahn condition was established on a sample of pure and highly crystalline kaolinite. ^{29}Si MAS NMR spectra were recorded at 79.5 MHz with a 6 s recycle delay and a 4 kHz spinning rate. ^{1}H → ^{29}Si CP/MAS NMR experiments were performed with a 2 s recycle delay, a 2 ms contact time, and a 5 kHz spinning rate. ^{1}H MAS NMR spectra were collected at 400.12 MHz using a single-pulse sequence with a $\pi/2$ pulse and a 5 s recycle delay. Two hundred scans were accumulated to record the ^{1}H spectra. ^{1}H/^{27}Al TRAPDOR experiment was performed according to the method of Grey and Vega [17]. In the experiment, a spin echo pulse was applied to ^{1}H channel and aluminum was simultaneously irradiated during the first echo period. The spinning rate was set to 3.3 kHz. Single-pulse ^{13}C MAS NMR with ^{1}H decoupling (1pda) experiments was recorded with a 4 s recycle delay and a spinning

rate of 4 kHz. $^{1}H \rightarrow {}^{13}C$ CP/MAS experiments were performed with a 2 ms contact time and a 2 s recycle delay. A spatially selective composite pulses [18] was combined with conventional 1pda and CP pulse sequences in order to effectively suppress weak signals (background) from the spinning module. ^{1}H, ^{27}Al, ^{29}Si, ^{13}C chemical shifts were referenced to TMS, aqueous $Al(NO_3)_3$, TMS and hexamethylbenzene, respectively.

3. Results and discussion

3.1. ^{27}Al MAS and $^{1}H \rightarrow {}^{27}Al$ CP/MAS NMR

^{27}Al MAS NMR spectra are sensitive to the variation of zeolite structure. Aluminum species with different structure or different chemical environment will have different chemical shifts in ^{27}Al MAS NMR spectra [19]. Fig. 1 shows the ^{27}Al MAS NMR spectra of parent and tungsten modified HZSM-5 catalysts. Two main peaks, one at 53 ppm typically due to four-coordinate framework aluminum [20] and the other at 0 ppm arising from octahedral extra-framework aluminum [21], are present in the ^{27}Al MAS NMR spectrum of HZSM-5. With increasing W loadings, the signal intensity of extra-framework aluminum at 0 ppm increases slightly at the expense of the framework aluminum, and the line width of the former are gradually broadened. This implies that an interaction between W species and the framework aluminum is likely to occur, which will lead to the dealumination

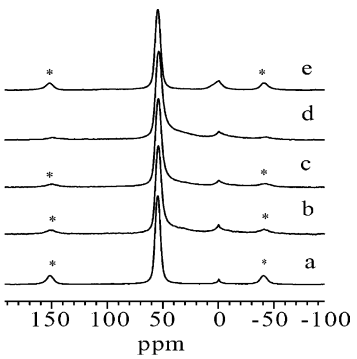

Fig. 1. ^{27}Al MAS NMR spectra of (a) HZSM-5; (b) 2W/HZSM-5; (c) 4W/HZSM-5; (d) 8W/HZSM-5; (e) 12W/HZSM-5. Asterisks denote spinning sidebands.

of the zeolite framework. This interaction was also observed in the case of Mo/HZSM-5 catalyst and other phase such as $Al_2(MoO_4)_3$ was present in the corresponding ^{27}Al MAS NMR spectra [9]. However, no signal of $Al_2(WO_4)_3$ is observed in our ^{27}Al MAS and $^{1}H \rightarrow {}^{27}Al$ CP/MAS NMR spectra. As revealed by previous studies [12], the W/HZSM-5 catalyst has a unique heat-resist performance at high temperature. For Mo/HZSM-5, it deactivates fast not only due to the Mo loss by sublimation but also because of the formation of $Al_2(MoO_4)_3$ which is detrimental to the reaction, especially at high temperature. Obviously, the two important factors leading to the deactivation of Mo/HZSM-5 are avoided in case of W/HZSM-5. Therefore, tungsten modified catalysts have a longer catalyst lifetime and keep nearly unchanged high activity for methane dehydroaromatization after regeneration.

After the introduction of W species, a broad peak between 0 and 50 ppm appears in the ^{27}Al NMR spectra of the 2W/HZSM-5, 4W/HZSM-5 and 8W/HZSM-5 catalysts. The assignment of the broad peak is a matter of dispute in the past 20 years. Some authors [22,23] attributed this signal to the distorted four-coordinate framework aluminum while others [24] ascribed it to five-coordinate extra-framework aluminum. Recently, Fyfe et al. [25] gave a clear assignment of a broad peak at about 30 ppm in ^{27}Al NMR spectra of USY by high-field solid-state MAS and MQMAS NMR techniques. It was apparent that the broad peak observed in the spectrum at 104.26 MHz had contributions from both tetrahedral and five-coordinate aluminum. van Bokhoven et al. [26] attributed a very broad peak between 40 and 50 ppm in ^{27}Al NMR spectrum of La(x)NaY to distorted four-coordinate framework aluminum on the basis of MQMAS NMR results. It is obvious that only MQMAS NMR can give a correct assignment of the broad peak. We tried to carry out ^{27}Al 3QMAS NMR spectrum of the 8W/HZSM-5 catalyst but did not obtained the corresponding signal of the broad peak, probably because of its relatively low concentration. So it is difficult to determine if the broad peak in our ^{27}Al NMR spectra is from distorted four-coordinate framework or five-coordinate extra-framework aluminum, or from the both of them. However, according to our ^{29}Si NMR spectra (see Table 1), the changes of the Si/Al ratios are relatively small in the series

Table 1
Concentration of Brönsted acid sites, silanols and extra-framework Al–OH of parent and tungsten modified HZSM-5 zeolites

Catalysts	Brönsted acid site (%)[a]	Nonframework Al–OH (%)[a]	Silanol (%)[a]	Si/Al ratio[b]
HZSM-5	100	100	100	29.1
2W/HZSM-5	91	113	86	29.6
4W/HZSM-5	81	139	79	31.6
8W/HZSM-5	80	141	75	32.1
12W/HZSM-5	78	165	59	32.4

[a] Determined by ^{1}H MAS NMR.
[b] Determined by ^{29}Si MAS NMR.

samples (from 29.1 to 32.4), it is more reasonable to assign the broad peak to distorted four-coordinate framework aluminum. If we attribute the broad peak to five-coordinate extra-framework Al, the apparent dealumination shown by ^{27}Al NMR seems to be greater if we consider the integral of the broad peak.

It should be noted that the broad peak between 0 and 50 ppm is absent in the ^{27}Al NMR spectrum of the 12W/HZSM-5 samples. This is probably due to the strong interaction between W species and framework aluminum, which leads to dealumination instead of distortion of the zeolite framework (an increase of the six-coordinate extra-framework Al). It can be expected that distortion of zeolite framework is predominant at low W loadings while only dealumination proceeds at high W loadings. We also recorded the ^{27}Al NMR spectrum of a 16W/HZSM-5 sample and did not find the presence of the broad peak (not shown).

$^{1}H \rightarrow {}^{27}Al$ CP/MAS NMR measurement can give the information about the aluminum that is associated with hydroxyl species, and some of the ^{27}Al signal will be selectively enhanced in the CP/MAS NMR experiments. $^{1}H \rightarrow {}^{27}Al$ CP/MAS spectra of parent HZSM-5 zeolite and W/HZSM-5 catalysts with different W loadings are displayed in Fig. 2. After the cross-polarization, the signal at 0 ppm and that between 0 and 50 ppm, which are assigned to six-coordinate and distorted four-coordinate framework aluminum, respectively, are greatly enhanced, indicating that these aluminum species are in close proximity to the hydroxyl groups.

^{29}Si MAS and $^{1}H \rightarrow {}^{29}Si$ CP/MAS NMR ^{29}Si MAS and $^{1}H \rightarrow {}^{29}Si$ CP/MAS NMR spectra are shown in Figs. 3 and 4, respectively. Four signals can be resolved by deconvoluting the corresponding spectra. Weak signal at −103 ppm is assigned to [Si(OH)(OSi)$_3$] (silanol) group [27], and the signals at −113 and −117 ppm are attributed to crystallographically inequivalent sites of Si(0Al) group [28]. The signal at −107 ppm is assigned to Si(1Al) group. Framework Si/Al ratio can be calculated from

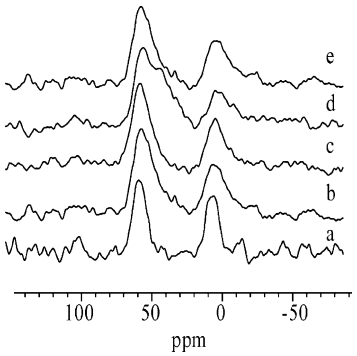

Fig. 2. $^{1}H \rightarrow {}^{27}Al$ CP/MAS NMR spectra of (a) HZSM-5; (b) 2W/HZSM-5; (c) 4W/HZSM-5; (d) 8W/HZSM-5; (e) 12W/HZSM-5.

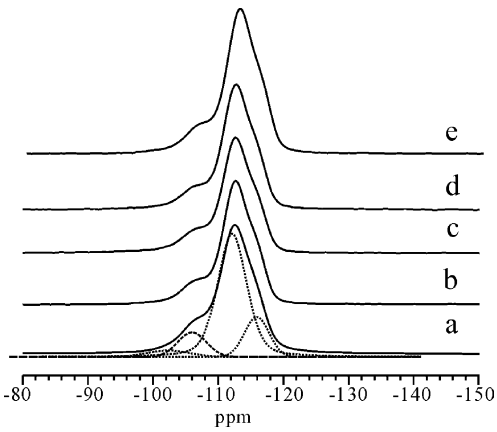

Fig. 3. ^{29}Si MAS NMR spectra of (a) HZSM-5; (b) 2W/HZSM-5; (c) 4W/HZSM-5; (d) 8W/HZSM-5; (e) 12W/HZSM-5.

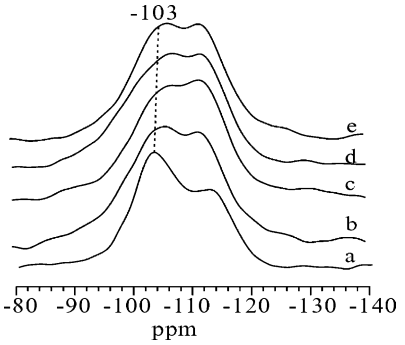

Fig. 4. $^{1}H \rightarrow {}^{29}Si$ CP/MAS NMR spectra of (a) HZSM-5; (b) 2W/HZSM-5; (c) 4W/HZSM-5; (d) 8W/HZSM-5; (e) 12W/HZSM-5.

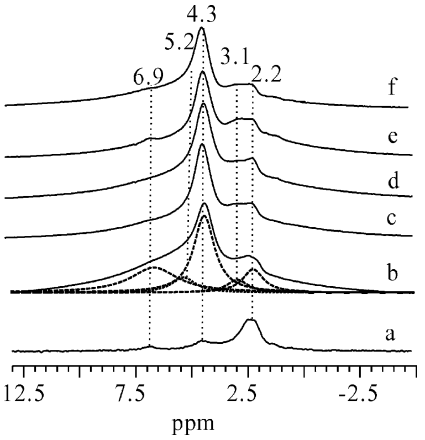

Fig. 5. $^{1}H/^{27}Al$ TRAPDOR spectrum of (a) HZSM-5; ^{1}H MAS NMR spectra deconvolution of (b) HZSM-5; (c) 2W/HZSM-5; (d) 4W/HZSM-5; (e) 8W/HZSM-5; (f) 12W/HZSM-5.

the individual peak areas in the ^{29}Si MAS NMR spectra [28] and the calculated results are listed in Table 1. Increasing the W loadings causes an increase of framework Si/Al ratios, implying that introduction of W species results in the dealumination of HZSM-5 and the more the W loading, the more intense the dealumination. This trend is consistent with the results of our ^{27}Al MAS NMR spectra.

The enhancement of the signal at −103 ppm in the corresponding $^{1}H \rightarrow {}^{29}Si$ CP/MAS NMR spectra suggests that it can be assigned to the silanol groups. As shown in Fig. 4, the concentration of silanols slightly decreases with increase of the W loading. This is due to the interaction between W species and silanols.

3.2. ^{1}H MAS and $^{1}H\{^{27}Al\}$ TRAPDOR NMR

^{1}H MAS NMR can give the direct information about the hydroxyl groups in zeolite. Fig. 5 shows the ^{1}H MAS NMR spectra of parent and W loaded HZSM-5 catalysts. Five resonances can be resolved (Fig. 5b) in ^{1}H MAS NMR spectra of HZSM-5. Signals at 2.2 and 3.1 ppm can be assigned to silanols and extra-framework Al–OH groups [29], respectively. Signal at 4.3 ppm is due to bridge hydroxyl group (Brönsted acid sites). As proposed by Beck et al [30], the broad peak at 6.9 ppm is assigned to a second kind of Brösted acid sites. The weak peak at 5.2 ppm arises from a third kind of Brönsted acid sites, which is located in the small cavities of HZSM-5 zeolite [31]. In order to confirm the assignment, $^{1}H\{^{27}Al\}$ TRAPDOR NMR experiment is carried out. As shown in Fig. 5a, under ^{27}Al irradiation, the signals at 3.1, 4.3, 5.2 and 6.9 ppm are significantly suppressed, indicating that the first four protons are in close proximity with aluminum atoms. The decrease of ^{1}H signals intensity with the increase of the W loadings suggest that condensation reaction between the W species and the various hydroxyl groups in the HZSM-5 occurs in the process of impregnation and calcination of the catalyst. However, the extent of condensation is much less than that in the case of Mo/HZSM-5 catalyst [31]. For example, for a 10Mo/HZSM-5, only 2% silanol groups, 25% Brönsted acid sites and 13% extra-framework Al–OH groups remain compared with the parent HZSM-5 after the introduction of Mo species, showing a preferential reaction between Mo species and silanols groups. For the 12W/HZSM-5 samples, however, 59% silanol groups and 78% Brönsted acid sites remain (see Table 1), while the concentration of extra-framework Al–OH groups increase by 65%. The less extent of the decrease of Brönsted acid sites and silanols in W/HZSM-5 than in Mo/HZSM-5 is likely due to two factors: one is the less uniform distribution of the W species on the surface of the zeolite, the other is the relatively weaker interaction between the W species and the various hydroxyl groups. The increase of the Al–OH concentration is partially due to the dealumination of zeolite framework and partially arises from the less condensation reaction between the W species and the extra-framework

hydroxyl groups, which is confirmed by the ^{27}Al MAS and $^{1}H \rightarrow {}^{27}Al$ CP/MAS NMR spectra. In the case of the Mo/HZSM-5 catalyst, Mo species is inclined to react with extra-framework aluminum and generate $Al_2(MoO_4)_3$ and the more the Mo loading, the more the reaction, which is responsible for the decrease of Al–OH groups.

Early study [32] has shown that most (>90%) of Brönsted acid sites are located on the internal surface of zeolite HZSM-5, so it is apparent that parts of W species have diffused into the internal channels and interacted with some Brönsted acid sites. As a bifunctional catalyst, the cooperation of the W species in/on the zeolite and the remaining Brönsted acid sites is responsible for the high activity of methane converting to aromatics. Previous works [33–35] have proved that the properties of the acidity of zeolite, such as strength, concentration and location of acid sites, significantly affect the activity of the catalyst and the distribution of products. By adding some metal ions such as Mg^{2+} and Li^{+} into W/HZSM-5 [12], which eliminates most of strong Brönsted acid sites and generates new medium–strong acid sites, the W/HZSM-5 catalysts appear to be a better catalytic performance. Therefore, how to optimize the Brönsted acidity and W species loadings so as to improve the activity and suppress the formation of the coke, is the further direction of study for this promising catalyst.

3.3. ^{13}C MAS and $^{1}H \rightarrow {}^{13}C$ CP/MAS NMR

By observing of products adsorbed on the surface of the catalysts, we can obtain more direct information about what happens on the surface of the catalyst in the process of the reaction than that by detecting off line gas phase products. Fig. 6 shows the ^{13}C MAS NMR spectra of methane reaction on 4W/HZSM-5 at different temperatures. Adsorption of methane on 4W/HZSM-5 at room temperature without any thermal treatment, there is a single peak (−8 ppm) of adsorbed methane in the ^{13}C MAS spectrum (Fig. 6a). After heating to 873 k for 1 h (Fig. 6b), the intensity of methane signal decreases, and a new signal at 126 ppm due to CO_2 appears, while in the corresponding CP spectrum (not shown), no other signal except for that from methane can be detected. Consumption of methane and the formation of CO_2 indicate that a partial reduction reaction of W^{6+} to W^{5+} happens

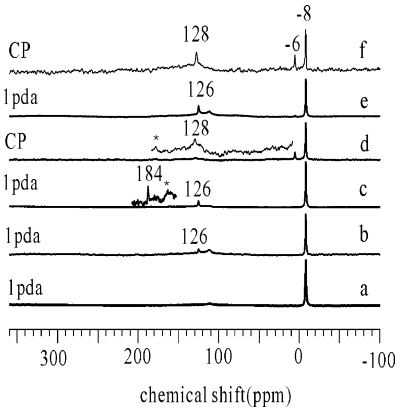

Fig. 6. ^{13}C MAS NMR spectra of methane (^{13}C, 99%) reaction on W/HZSM-5 at (a) room temperature, 1 pulse with ^{1}H decoupling (1pda); (b) 873 K for 1 h, 1pda; (c) 973 K for 30 min, 1pda; (d) 973 K for 30 min, CP; (e) 1073 K for 1 h, 1pda; (f) 1073 K for 1 h, CP. The spectra were recorded at room temperature. Asterisks denote spinning sidebands. The weak signals at ca. 112 ppm are due to the background from the spinning module.

in/on catalyst at 873 K. Zhang and co-workers [12] also observed this reduction process at this temperature by H_2-TPR. After reaction running at 973 K for 30 min, as shown in Fig. 6c, the signal of CO_2 increases, and a new peak at 184 ppm appears, which is absent in the corresponding CP spectrum. According to its chemical shift, we attribute the new signal to CO. The formation of CO suggests that W species has been reduced to a lower oxidation valence state, such as W^{4+}, by methane at 973 K.

$$WO_3 + CH_4 \rightarrow WO_x + CO + CO_2 + H_2O$$

In corresponding CP spectrum, the signals of products such as ethane (6 ppm) and benzene (128 ppm) are present, implying that methane has been activated with the formation of W^{4+} oxide. Therefore, the W^{4+} oxide is likely to be the active phase for the initial activation of methane. This agrees well with the results of Zeng and co-workers [12] who observed the reduction of W species by EPR in different W/HZSM-5 catalysts prepared by impregnation $(NH_4)_2WO_4$ solution with different pH values. For a catalyst impregnated in a solution with pH values of 8–9, W species existed in form of tetrahedral coordination $(WO_4)^{2-}$ and was difficult to be reduced to W^{4+} state, and thus the catalyst had little activity in methane activation. However, for

a catalyst prepared in a solution of pH values of 2–3, W species was transformed into octahedral $(WO_6)^{n-}$ and was easy to be reduced to W^{4+} species, and thus the catalyst had a good catalytic performance.

Recently, Ding et al. [36] reported the observation the WC_x cluster in W/HZSM-5 catalyst (prepared by solid exchange method) after 1 h reaction by absorption near-edge spectra (XANES) and concluded that the WC_x species was responsible for the initial activation of methane. But in all of our ^{13}C MAS NMR experiments, we have not detected any signal of carbide tungsten, even after 1 h reaction at 1073 K (Fig. 6e). Lunsford and co-workers [37] gained the same results. They did not discover signal of carbide tungsten by XPS for a W/HZSM-5 catalyst after 16 h reaction. Using ^{13}C MAS NMR, we could observe the signal from carbide molybdenum at ca. 274 ppm for a 6Mo/HZSM-5 catalyst after methane reaction at 973 K for 30 min [38]. Therefore, in the case of the W/HZSM-5 catalysts prepared by wetness impregnation, W^{4+} oxide probably acts as active site for the activation of methane.

4. Conclusions

The present results demonstrate that, for the controlled impregnation-prepared W/HZSM-5 catalyst, introduction of the W species onto HZSM-5 zeolite leads to distortion and dealumination of zeolite framework. Some of W species diffuse into the internal channels of the zeolite and they interact with the Brönsted acid sites and the silanols, resulting in the removal of the corresponding hydroxyl groups during the impregnation and calcination of the catalyst. Cooperation of W species and Brönsted acid sites is responsible for the methane conversion reaction. W^{4+} oxide reduced by methane in the induction period is likely to be the active metal site for the initial activation of methane on the W/HZSM-5 catalysts.

Acknowledgements

We are very grateful to the National Natural Science Foundation of China for financial support (29973058 and 20173072), and to Prof. T.H. Chen of Nankai University for providing HZSM-5 zeolite.

References

[1] R.H. Crabtree, Chem. Rev. 95 (1995) 987.
[2] L. Wang, L. Tao, M. Xie, G. Xu, J. Huang, Y. Xu, Catal. Lett. 21 (1993) 35.
[3] D. Wang, J.H. Lunsford, M.P. Rosnek, J. Catal. 169 (1997) 347.
[4] W. Liu, Y. Xu, J. Catal. 185 (1999) 386.
[5] S. Liu, L. Wang, R. Ohnishi, M. Ichikawa, J. Catal. 181 (1999) 175.
[6] P. Meriaudeau, L.V. Tiep, V.T.T. Ha, C. Naccache, G. Szabo, J. Mol. Catal. A 144 (1999) 469.
[7] F. Solymosi, A. Erdohelyi, A. Szoke, Catal. Lett. 32 (1995) 43.
[8] D. Ma, Y. Shu, X. Bao, Y. Xu, J. Catal. 189 (2000) 314.
[9] W. Zhang, D. Ma, X. Han, Y. Xu, X. Bao, J. Catal. 188 (1999) 393.
[10] D. Ma, Y. Shu, W. Zhang, X. Han, Y. Xu, X. Bao, Angew. Chem. Int. Ed. 39 (2000) 2928.
[11] Y. Xu, L. Lin, Appl. Catal. A 188 (1999) 53.
[12] J. Zeng, Z. Xiong, H. Zhang, G. Lin, K.R. Tsai, Catal. Lett. 53 (1998) 119;
Z. Xiong, L. Chen, H. Zhang, Catal. Lett. 74 (2001) 227;
Z. Xiong, H. Zhang, G. Lin, J. Zeng, Catal. Lett. 74 (2001) 233.
[13] M. Hunger, J. Weitkamp, Angew. Chem. Int. Ed. 40 (2001) 2955.
[14] M. Hunger, Catal. Rev.-Sci. Eng. 39 (1997) 345.
[15] M.W. Anderson, J. Klinowski, Nature 339 (1989) 200.
[16] J.F. Haw, J.B. Nicholas, W. Song, F. Deng, Z. Wang, T. Xu, C.S. Hengghan, J. Am. Chem. Soc. 122 (2000) 4763.
[17] C.P. Grey, A.J. Vega, J. Am. Chem. Soc. 117 (1995) 8232.
[18] A.D. Bax, J. Magn. Reson. 65 (1985) 142.
[19] J. Rocha, S. Carr, J. Klinowsli, Chem. Phys. Lett. 187 (1991) 401.
[20] J. Rocha, J. Klinowsli, J. Chem. Soc., Chem. Commun. 1991 (1121).
[21] L.B. Alemany, G.W. Kirker, J. Am. Chem. Soc. 108 (1986) 6158.
[22] A. Samoson, E. Lippma, G. Engelhardt, U. Lohse, H.G. Jerschkewitz, Chem. Phys. Lett. 34 (1987) 589.
[23] M.J. Remy, D. Stanica, G. Poncelet, E.J.P. Feijen, P.J. Grobet, A.J. Martens, P.A. Jacobs, J. Phys. Chem. 100 (1996) 12440.
[24] G.J. Ray, A. Samason, Zeolite 13 (1993) 410;
D. Coster, A.L. Blumenfield, J.J. Fripiat, J. Phys. Chem. 98 (1994) 6201.
[25] C.A. Fyfe, J.L. Bretherton, L.Y. Lam, Chem. Commun. 2000 (1575).
[26] J.A. van Bokhoven, A.L. Roest, D.C. Koningsberger, J.T. Miller, G.H. Nachtegaal, A.P.M. Kentgens, J. Phys. Chem. B 104 (2000) 6743.
[27] E. Brunner, H. Ernst, D. Freude, T. Frohlish, M. Hunger, H.J. Pfeifer, J. Catal. 127 (1991) 34;
C.A. Fyfe, G.C. Gobbl, G.J. Kennedy, J.D. Graham, R.S. Ozubko, W.J. Murphy, A. Bothner, J. Dadok, A.S. Che, Zeolite 5 (1985) 179.

[28] G. Engelhard, D. Michel, High-Resolution Solid State NMR of Silicates and Zeolite, Wiley, New York, 1987.
[29] H. Hunger, D. Freude, H. Pfeiffer, J. Chem. Soc., Faraday Trans. 87 (1991) 657.
[30] L.W. Beck, J.F. Haw, J. Phys. Chem. 99 (1995) 1076.
[31] F. Deng, Y. Du, C. Ye, J. Wang, T. Ding, H. Li, J. Phys. Chem. 99 (1995) 15208.
[32] D. Ma, W. Zhang, Y. Shu, X. Liu, Y. Xu, X. Bao, Catal. Lett. 65 (2000) 155.
[33] M. Guisnet, Acc. Chem. Rev. 23 (1990) 392.
[34] P. Ganiti, A. Gervasini, A. Auroud, J. Catal. 150 (1994) 274.
[35] R.S. Drago, S.C. Dias, M. Torrealda, L. Lima, J. Am. Chem. Soc. 119 (1997) 4444.
[36] W. Ding, G.D. Meitzner, D.D. Marler, E. Iglesia, J. Phys. Chem. B 105 (2001) 3928.
[37] B.M. Weckhuysen, D. Wang, M.P. Rosynek, J.H. Lunsford, J. Catal. 175 (1998) 347.
[38] J. Yang, D. Ma, F. Deng, Q. Luo, M. Zhang, X. Bao, C. Ye, Chem. Commun. (2002) 3046.